Hindawi Publishing Corporation
Advances in Chemistry
Volume 2014, Article ID 506851, 12 pages
http://dx.doi.org/10.1155/2014/506851

Research Article

Cobalt(II) and Manganese(II) Complexes of Novel Schiff Bases, Synthesis, Charcterization, and Thermal, Antimicrobial, Electronic, and Catalytic Features

Selma Bal and Sedat Salih Bal

Chemistry Department, Faculty of Arts and Science, Kahramanmaras Sutcu Imam University, Avsar Kampusu, 46100 Kahramanmaras, Turkey

Correspondence should be addressed to Selma Bal; selmadagli9@hotmail.com

Received 6 June 2014; Accepted 28 July 2014; Published 21 August 2014

Academic Editor: Alessandro D'Annibale

Carbazoles containing two new Schiff bases (Z,Z)-N,N′-bis[(9-ethyl-9*H*-carbazole-3-yl)methylene]propane-1,3 diamine (L^1) and (Z,Z)-N,N′-bis[(9-ethyl-9*H*-carbazole-3-yl)methylene]-2,2-dimethylpropane-1,3-diamine (L^2) and their Co(II) and Mn(II) complexes were synthesized and characterized using various spectroscopic methods and thermal analysis, which gave high thermal stability results for the ligands and their cobalt complexes. The title compounds were examined for their antimicrobial and antifungal activities, which resulted in high activity values for the ligands and their manganese complexes. Oxidation reactions carried out on styrene and cyclohexene revealed that the complex compounds were the most effective catalysts for styrene oxidation, giving good selectivities than those of cyclohexene oxidation. Electronic features of the synthesized compounds were also reported within this work.

1. Introduction

Schiff bases and their complexes have been and are being employed to many reactions in synthetic chemistry. In particular, the oxidation of alkenes is important intermediate to get new, industrially important chemicals for both organic synthesis and pharmaceutical industry. Catalytic transformations of hydrocarbons into valuable oxygenated derivatives such as alcohols, aldehydes, and epoxides using peroxides as oxidants have been extensively studied over the last few decades [1–5]. In particular, the catalysis of alkene oxidation by soluble transition metal complexes is of great interest in both biomimetic chemistry and synthetic chemistry [6]. So far various Schiff base complexes have been employed to catalytic oxidation of olefins to epoxides and aldehydes, and it has been proved that many Schiff base complexes gave improved results as catalysts for these kinds of oxidation reactions [7–20]. In our research, the synthesized Schiff base complexes have been searched for their potential use as catalysts in oxidation reactions for both cyclohexene and styrene. Not only for these oxidation reactions but also for many kinds, it is important to use eco-friendly with easy recoverability oxidants such as H_2O_2 and air. It is also important that the catalysts are thermally stable enough to carry out these kinds of reactions which generally require elevated temperatures [21, 22].

In addition their catalytic activities, various Schiff bases have also been examined for their biological activities in many previous studies [23–25]. This interest comes from the fact that their metal complexes can be used as antimicrobial, antifungal, and antitumor agents [26–28].

In previous studies various carbazoles containing Schiff bases and their coordination compounds have been synthesized, characterized, and examined for their different features such as luminescence, thermal property [29–33], biological activity [34], and electrochemical and optical behaviour [35–37] and for their use as Langmuir-Blodgett film [38].

We report here total synthesis, spectral and thermal characterization of two carbazole derived novel Schiff bases and their copper(II) and manganese(II) complexes, their

thermal, electrochemical, antimicrobial features, and their effect as catalysts in the oxidation reactions of cyclohexene and styrene.

2. Experiment

2.1. Materials and Instrumentation. 9-Ethylcarbazole, phosphorus(V) oxychloride, 1,3-diaminopropane, and 2,2-dimethyl-1,3-diaminopropane, all the solvents used, and acetate salts of copper(II) and manganese(II) were purchased from Sigma Aldrich. Nuclear magnetic resonance spectra of the synthesized ligands were recorded on a Bruker AV 400 MHz spectrometer in the solvent $CDCl_3$. Infrared spectra were obtained using KBr discs on a Shimadzu 8300 FTIR spectrophotometer in the region of 400–4000 cm^{-1}. Ultraviolet spectra were run in ethanol on a Schimadzu UV-160A spectrophotometer. Magnetic measurements were carried out by the Gouy method using $Hg[Co(SCN)_4]$ as a calibrant. Molar conductances of the ligands and their transition metal complexes were determined in MeOH ($\sim 10^{-3}$) at room temperature using a Jenway Model 4070 conductivity meter. Mass spectra of the ligand were recorded on a LC/MS APCI Agilent 1100 MSD spectrophotometer. The oxidation products were analyzed with a gas chromatograph (Shimadzu, GC-14B) equipped with a SAB-5 capillary column and a flame ionization detector. Elemental analyses were performed on a LECO CHNS 932 elemental analyzer and the metal analyses were carried out on an Ati Unicam 929 Model AA spectrometer in solutions prepared by decomposing the compounds in aqua regia and subsequently digesting them in concentrated HCl. Thermal analyses of synthesized ligands and their metal complexes were carried out on a Perkin-Elmer Thermogravimetric Analyzer TG/DTA 6300 instrument under nitrogen atmosphere between the temperature ranges 30°C and 988°C at a heating rate of 10°C/min. Cyclic voltammetry was performed using IviumStat electrochemical workstation equipped with a low current module (BAS PA-1) recorder.

2.2. Synthesis of 9-Ethyl-9H-carbazole-3-carbaldehyde. Formulation of 9-ethylcarbazole was done by using Vilsmeier formulating agents DMF and $POCl_3$. Inside a fume cupboard, DMF (32 mL, 0.4 mol) was put into a 250 mL round-bottom flask placed in an ice bath. Over DMF at 0°C 32 mL (0.32 mol) $POCl_3$ was added dropwise through a dropping funnel. Resulting solution was stirred at room temperature for 2 hours. To the stirring mixture, 9-ethyl-9*H*-carbazole (8 g, 0.04 mol) dissolved in 32 mL DMF was slowly added. The reaction mixture was heated at 80°C and left stirring for 24 hours. The resulting dark coloured mixture was poured into slurry of crushed ice and water (250 mL). The precipitate was washed with water and extracted by $CHCl_3$ and then washed with *n*-hexane. The dirty yellow precipitate was subjected to flash column chromatography with the eluent of ethyl acetate/hexane (1 : 10). Vilsmeier reaction always gives both mono- and dialdehyde of the formulated carbazole [39, 40]. The monoaldehyde was the first product eluated as yellowish-white crystals. The dialdehyde obtained was white solid. TLC chromatography, elemental analysis, and spectral data confirm the purity and structure of synthesized mono- and dialdehyde products. Monoaldehyde 9-ethyl-9*H*-carbazole-3-carbaldehyde: yield: 40%. m.p.: 85–87°C. UV-Vis (ethanol) (λ_{max}, nm) (ε, $M^{-1}\,cm^{-1}$): 202(50000), 210(80000), 226(30000), 264(36000), 284(95000). FT-IR (KBr, cm^{-1}): 1591(w), 1622(w), 2850(w), 2922(w)(Ar-H and C-H); 1681(s)(CHO). ^{1}H NMR(400 MHz, $CDCl_3$): 10.1(CHO), 8.6 (H-4, d, J = 1.3), 8.16 (H-5, brd, J = 7.8), 8.02 (H-2, dd, J = 8.5&1.58), 7.46 (H-1&H-8, d, J = 8.4), 7.56 (H-7, dt, J = 8.2&1.2), 7.35 (H-6, dt, J = 8.0&1.03), 4.39 (2H-14, q, J = 7.2), 1.47 (3H-15, t, J = 7.2). ^{13}C NMR(400 MHz, $CDCl_3$): 191.8(CHO), 127.2(C-1), 126.8(C-2), 128.5(C-3), 124.01(C-4), 120.8(C-5), 120.3(C-6), 108.7(C-7), 109.2(C-8), 143.5(C-10), 123.1(C-11), 123.0(C-12), 140.7(C-13), 37.9(C-14), 13.9(C-15). Mass spectrum (LC/MS APCI): m/z 223.7 $[M]^+$.

2.3. Synthesis of the Ligands (Z,Z)-N,N′-Bis[(9-ethyl-9H-carbazol-3-yl)methylene]propane-1,3-diamine (L^1) and (Z,Z)-N,N′-Bis[(9-ethyl-9H-carbazol-3-yl)methylene]-2,2-dimethylpropane-1,3-diamine (L^2). Inside a 100 mL round-bottom flask, 0.45 g (2 mmol) 9-ethyl-9*H*-carbazole-3-carbaldehyde was put and dissolved in enough amount of ethanol. Over this, 0.1 g (1 mmol) diamine was added dropwise. The resulting solution was heated under reflux for four hours and left overnight. The white precipitate was recrystallized from ethanol (Figure 1).

2.3.1. (Z,Z)-N,N′-Bis[(9-ethyl-9H-carbazole-3-yl)methylene]-propane-1,3-diamine (L^1). Yield: 80%, m.p.: 167°C, elemental analysis found % (calculated %): C 82.34(81.78) H 6.80(6.66) N 12.01(11.56). UV-Vis (ethanol) (λ_{max}, nm) (ε, $M^{-1}\,cm^{-1}$): 216(175000), 250(105000), 266(120000), 296(210000), 310(161000). FT-IR (KBr, cm^{-1}): 2843(w), 2920(w), 2971(w), 1598(w)(Ar-H and C-H); 806(s), 740(s)(Ar-H) 1637(s)(imine). Mass spectrum (LC/MS APCI): m/z 485.2 $[M+1]^+$, 280.1 $[M-204.53]$, which arises from the loss of ten hydrogen and one carbazole units leaving $C_{19}H_{10}N_3$. ^{1}H NMR(400 MHz, $CDCl_3$): 7.44 (H-1&H-8, d, J = 8.5), 7.92 (H-2, dd, J = 8.5&1.5), 8.49 (H-4, d, J = 1.4), 8.15 (H-5, d, J = 7.6), 7.28 (H-6, dt, J = 1.2&7.6), 7.51 (H-7, dt, J = 1.2&7.1), 4.41 (H-14, q, J = 7.2), 1.47 (H-15, t, J = 7.2), 3.84 (H-16&H-18, q, J = 7), 2.26 (H-17, m, J = 7), 8.5 (imine, s). ^{13}C NMR(400 MHz, $CDCl_3$): 126.03(C-1), 125.9(C-2), 127.7(C-3), 123.1(C-4), 120.7(C-5), 119.4(C-6), 108.5(C-7), 108.7(C-8), 141.5(C-10), 127.2(C-11), 124.0(C-12), 140.5(C-13), 37.7(C-14), 13.8(C-15), 59.5(C-16&C-18), 32.3(C-17), 162.06(imine).

2.3.2. (Z,Z)-N,N′-Bis[(9-ethyl-9H-carbazol-3-yl)methylene]-2,2-dimethylpropane-1,3-diamine (L^2). Yield: 75%, m.p.: 115°C, elemental analysis found % (calculated %): C 82.11 (81.99) H 7.530(7.08) N 11.01(10.93). UV-Vis (ethanol) (λ_{max}, nm) (ε, $M^{-1}\,cm^{-1}$): 268(115000), 300(78000), 306(61000), 334(99000). FT-IR (KBr, cm^{-1}): 2973(w), 2949(w), 2867(w), 2821(w), 1595(w) (Ar-H and C-H); 809(s), 747(s)(Ar-H) 1646(s)(imine). Mass spectrum (LC/MS APCI): m/z 514.3

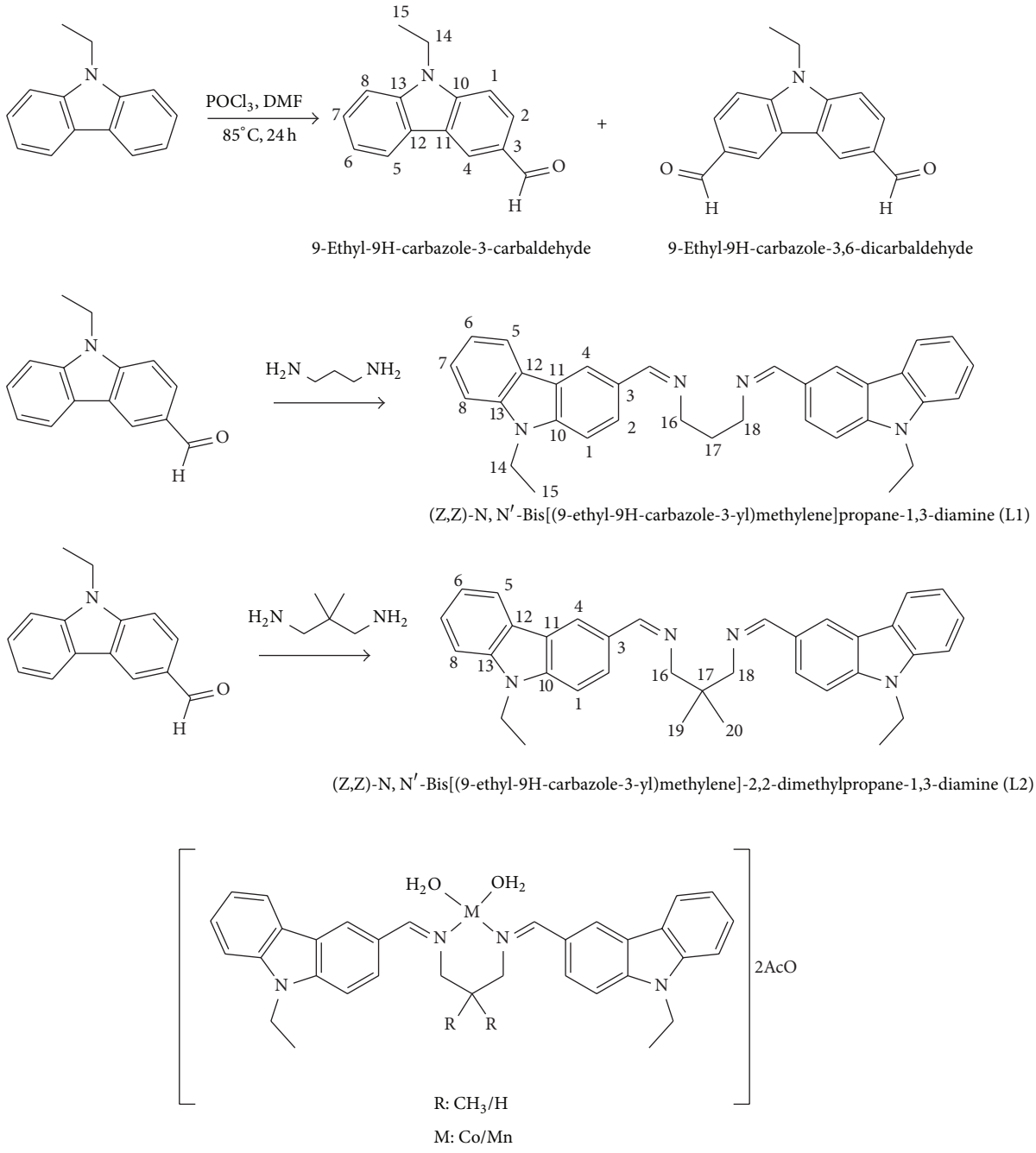

Figure 1: Synthesis scheme of the synthesized compounds and the proposed structure for the metal complexes.

$[M + 1]^+$, 308.1 [M − 204], which arises from the loss of ten hydrogen and one carbazole units leaving $C_{21}H_{14}N_3$. ^{1}H NMR(400 MHz, $CDCl_3$): 7.44(H-1&H-8, d, J = 8.4), 7.99 (H-2, dd, J = 8.5&1.5), 8.49 (H-4, d, J = 1.3), 8.16 (H-5, d, J = 7.6), 7.29 (H-6, dt, J = 1.1&7.1), 7.53 (H-7, dt, J = 1.1&7.0), 4.42 (H-14, q, J = 7.2), 1.48 8H-15, t, J = 7.2), 3.67 (H-16&H-18, s), 1.2 (H-19&H-20, s), 8.48 (imine, s). ^{13}C NMR(400 MHz, $CDCl_3$): 125.9(C-1), 125.9(C-2), 128.0(C-3), 123.05(C-4), 120.8(C-5), 119.4(C-6), 108.5(C-7), 108.7(C-8), 141.4(C-10), 127.2(C-11), 123.1(C-12), 140.7(C-13), 37.7(C-14), 13.9(C-15), 58.2(C-16&C-18), 37.3(C-17), 24.8 (C-19&C-20).

2.4. Synthesis of Complex Compounds. The ratio of the metal salts and the ligands was taken as 1 : 1 (Figure 1). A solution of the metal salt (1 mmol) in 15 mL absolute ethanol was added into the solution of the ligand L^1/L^2 (1 mmol) in 15 mL ethanol. The mixtures were stirred under reflux overnight. The precipitates were filtered, washed with distilled water to get rid of the excess salt, and dried in vacuum.

2.4.1. Cobalt(II) Complex of L^1. $[CoL^1(H_2O)_2]\cdot 2AcO$ complex: ($C_{33}H_{36}CoN_4O_2$), brown coloured, yield: 72%, m.p.: 205.5°C, Elemental Analysis found % (calculated %):

C 63.65(63.38), H 6.71(6.26), N 9.66(9.67), Co 10.68(10.17). UV-Vis (ethanol) (λ_{max}, nm) (ε, $M^{-1}\,cm^{-1}$): 256(51000), 282(11600), 330(87000), 367(75000), 482(30000), 560(33000). FT-IR (KBr, cm^{-1}): 3350, 3220(O-H), 2972, 2822, 2745(Ar-H, C-H), 1575(imine), 439(M-N), 537(M-O). Λ_M ($\Omega^{-1}\,cm^2\,mol^{-1}$): 80.1, μ_{eff} B.M.: 4.35.

2.4.2. Manganese(II) Complex of L^1. $[MnL^1(H_2O)_2]\cdot 2AcO$ complex: ($C_{33}H_{36}MnN_4O_2$), brown coloured, yield: 64%, m.p.: 198°C, Elemental Analysis found % (calculated %): C 69.23(68.86), H 6.21(6.30), N 10.15(9.73), Mn 10.02(9.54). UV-Vis (ethanol) (λ_{max}, nm) (ε, $M^{-1}\,cm^{-1}$): 246(86000), 291(51000), 375(24000), 640(12000). FT-IR (KBr, cm^{-1}): 3342(O-H), 2847, 2730(Ar-H, C-H), 1589(imine), 481(M-N), 604(M-O). Λ_M ($\Omega^{-1}\,cm^2\,mol^{-1}$): 28.7, μ_{eff} B.M.: 5.85.

2.4.3. Cobalt(II) Complex of L^2. $[CoL^2(H_2O)_2]\cdot 2AcO$ complex: ($C_{35}H_{40}CoN_4O_2$), black coloured, yield: 60%, m.p.: 146.5°C, Elemental Analysis found % (calculated %): C 70.09(69.18), H 6.92(6.63), N 9.57(9.22), Co 10.01(9.70). UV-Vis (ethanol) (λ_{max}, nm) (ε, $M^{-1}\,cm^{-1}$): 230(120000), 284(61000), 384(43000), 620(10200). FT-IR (KBr, cm^{-1}): 3306(O-H), 2919, 2812(Ar-H, C-H), 1550(imine), 553(M-N), 654(M-O). Λ_M ($\Omega^{-1}\,cm^2\,mol^{-1}$): 67.3, μ_{eff} B.M.: 4.89.

2.4.4. Manganese(II) Complex of L^2. $[MnL^2(H_2O)_2]\cdot 2AcO$ complex: ($C_{33}H_{40}MnN_4O_2$), dark green coloured, yield: 54%, m.p.: 119°C, elemental analysis found % (calculated %): C 70.03(69.64), H 7.14(6.68), N 9.67(9.28), Mn 9.25(9.10). UV-V is (ethanol) (λ_{max}, nm) (ε, $M^{-1}\,cm^{-1}$): 265(90000), 395(71000), 567(14000). FT-IR (KBr, cm^{-1}): 3252(O-H), 2920, 2835(Ar-H, C-H), 1540(imine), 490(M-N), 601(M-O). Λ_M ($\Omega^{-1}\,cm^2\,mol^{-1}$): 35.2, μ_{eff} B.M.: 6.23.

2.5. Preparation of Microorganism Culture. The growth inhibitory activity of the synthesized compounds was tested against 4 gram negative, 4 gram positive bacteria (*Klebsiella pneumoniae* FMC 5, *Escherichia coli* DM, and *Enterobacter faecium* (clinic isolate) and *Enterobacter aerogenes* ATCC 13048, *Bacillus subtilis* IMG 22, *Bacillus megaterium* DSM 32, *Staphylococcus aureus* ATCC 25923, and *Streptococcus faecalis*) and 3 yeasts (*Candida albicans* ATCC 1023, *Candida utilis*, and *Saccharomyces cerevisiae* WET 136). These microorganisms were provided from Microbiology Laboratory Culture Collection, Department of Biology, Kahramanmaraş Sütçü İmam University, Turkey.

Antimicrobial activities of the compoundswere determined using the hollow agar. The bacteria were first incubated at 37 ± 0.1°C for 24 h in nutrient broth (Difco), and the yeasts were incubated in Sabouraud dextrose broth (Difco) at 25 ± 0.1°C for 24 h. The cultures of the bacteria and yeast were injected into the Petri dishes (9 cm) in the amount of 0.1 mL (McFarland OD: 0.5, 1.5×10^8 bacteria/mL and 1.5×10^6 yeast/mL) [38, 39, 41, 42]. Then, Mueller Hinton agar and Sabouraud dextrose agar (sterilized in a flask and cooled to 45–50°C) were homogeneously distributed onto the sterilized Petri dishes in the amount of 25 mL. Finally, 2 mg of each chemical compound dissolved in ethanol was placed inside the sterilised antibiotic discs. The prepared antibiotic discs were then placed in the bacterial medium.

Afterwards, the plates combined with the discs were left at 4°C for 2 h, the plates injected with yeast were incubated at 25 ± 0.1°C for 24 h, and ones injected with bacteria were incubated at 37 ± 0.1°C for 24 h. After 24 h, inhibition zones appearing around the disks were measured and recorded in mm [41–44].

2.6. Determination of Minimal Inhibitory Concentration (MIC). A broth microdilution broth susceptibility assay was used, as recommended by NCCLS, for the determination of the MIC of the ligand and the complexes and some reference components [38, 41]. All tests were performed in Mueller Hinton broth (MHB) supplemented with Tween 80 detergent (final concentration of 0.5% (v/v)), with the exception of the yeasts (Sabouraud dextrose broth (SDB) + Tween 80). Bacterial strains were cultured overnight at 37°C in MHB, and the yeasts were cultured overnight at 30°C in SDB. Geometric dilutions ranging from 200 to 2500 μg/mL of the compounds were prepared including one growth control (MHB + Tween 80) and one sterility control (MHB + Tween 80 + test oil). Test tubes were incubated under normal atmospheric conditions at 37°C for 24 h for bacteria and at 30°C for 48 h for the yeasts. The microbial growth was determined by turbidimetric methods.

2.7. Oxidation Procedure. A mixture of 1.10^{-3} mol catalyst, 20 mL solvent (CH_3CN), and 10 mmol cyclohexene/styrene was stirred under nitrogen atmosphere in a 50 mL round-bottom flask equipped with a condenser and a dropping funnel at room temperature for 30 min. Then 20 mmol hydrogen peroxide (30% in water) was added (catalyst : substrate : oxidant ratio is 1 : 10 : 20). The resulting mixture was then refluxed for 8 h under nitrogen atmosphere at 90°C. After filtration and washing with solvent, the filtrate was concentrated and then subjected to GC analysis. The yields were recorded as the GC yield based on the starting styrene or cyclohexene. The identity of the oxidation products was confirmed by GC-MS. A blank reaction was also carried out without any catalyst for both oxidation reactions.

3. Results and Discussion

3.1. IR and UV Spectra of the Ligands and the Complexes. IR spectrum of 9-ethyl-3-formylcarbazole revealed the characteristic weak C-H stretching bands belonging to aromatic rings at 1591 cm^{-1}, 1622 cm^{-1}, 2850 cm^{-1}, and 2922 cm^{-1}. The latter two bands might also be the C-H stretching frequencies generally observed for saturated methyl or methylene groups. The aromatic aldehyde was observed at 1681 cm^{-1}. Following the imine formation, this band was replaced for the imine stretching frequencies at 1638 cm^{-1} for L^1 and at 1646 cm^{-1} for L^2. In the IR spectra of L^1 and L^2, the weak bands between 2821 and 2973 cm^{-1} belong to weak aromatic and saturated C-H stretchings. The medium strength bands at 1598 cm^{-1} for L^1 and at 1595 cm^{-1} for L^2 belong to aryl-H vibrations. If we examine the substitution patterns of the

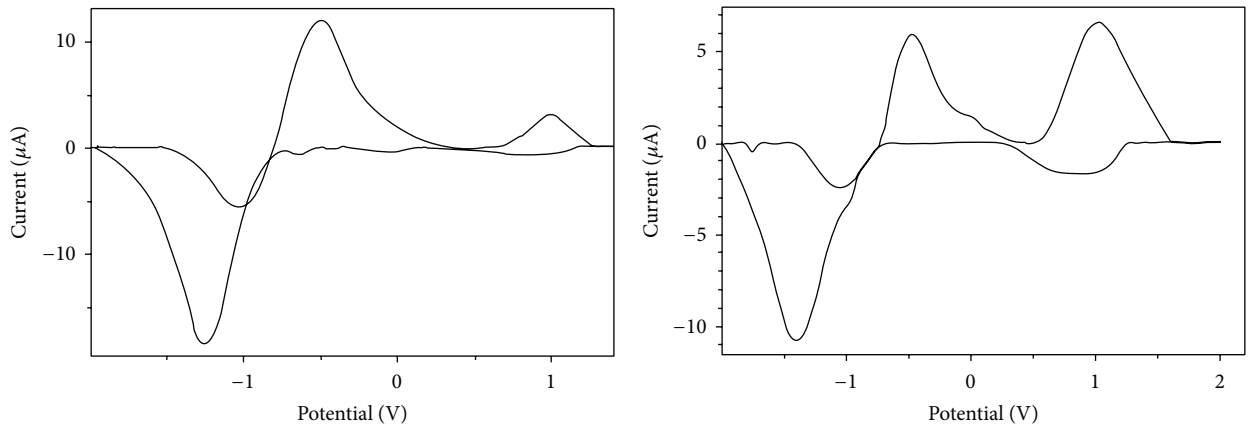

FIGURE 2: (a) Cyclic voltammogram of L^1 in the presence of 0.1 M NBu_4BF_4 in DMF solution at 1.10^{-3} M at 100 mVs^{-1}. (b) Cyclic voltammogram of L^1-Co in the presence of 0.1 M NBu_4BF_4 in DMF solution at 1.10^{-3} M at 500 mVs^{-1}.

benzene rings, we can say that one metadisubstituted (strong aryl-H vibrations at 806 cm^{-1} for L^1 and at 809 cm^{-1} for L^2) and one orthodisubstituted benzene ring (strong aryl-H vibrations at 740 cm^{-1} for L^1 and at 747 cm^{-1} for L^2) are present in our ligands.

Following the coordination, the imine frequencies recorded for the ligands were red shifted and appeared at around 1575 cm^{-1} for L^1-Co, 1589 cm^{-1} for L^1-Mn, 1550 cm^{-1} for L^2-Co, and 1540 cm^{-1} for L^2-Mn complexes as weak signals. All the coordination compounds showed coordinated water frequencies between 3252 and 3306 cm^{-1} [45]. The M-N stretching vibrations observed between 439 and 553 cm^{-1} proved that the nitrogens of the imine groups coordinate with the central metal atoms.

The UV spectra of all ligands and the complexes were taken in ethanol in the range between 200 nm and 700 nm. For the complex compounds the d-d transitions were observed between 560 nm and 640 nm, and the bands observed in the 395–367 nm range for these complexes can be attributed to the charge transfer bands from ligand to metal or from metal to ligand centre [46, 47]. The n-π^* and π-π^* transitions of the synthesized ligands and complexes were observed in 202–334 nm region. The O-H stretching frequencies in water molecules assisting in coordination were seen as broad singlets between 3306 cm^{-1} and 3350 cm^{-1} [45]. All the infrared and u.v. results are given in the experimental Sections 2.2–2.4. The magnetic moment values for cobalt complexes were recorded as 4.35 B.M. and 4.89 B.M., which are characteristic values for tetrahedral cobalt complexes [46, 47]. The manganese(II) complexes gave 5.85 B.M. and 6.23 B.M. values, indicating a high spin complex and suggesting tetrahedral geometry [48, 49].

3.2. Electrochemical Properties of the Synthesized Compounds. Cyclic voltammogram studies were run in DMF (1×10^{-3} M)–0.1 M NBu_4BF_4 as supporting electrolyte at 293 K. Electronic spectra of all the compounds were taken for scan rates 100, 250, 500, 750, and 1000 mVs^{-1} against an internal ferrocene-ferrocenium standard and we have obtained different oxidation and reduction processes for different scan rates. Examination of cv graphics of L^1 shows reversible oxidation-reduction processes for the scan rate 100 mVs^{-1} (Figure 2(a)) at 0.87 V(E_{pc}) and 0.88 V(E_{pa}) ($I_{pc} : I_{pa} = 1$) and for the scan rate 500 mVs^{-1} at 0.94 V(E_{pc}) and 1.04 V(E_{pa}) ($I_{pc} : I_{pa} \cong 1$). The quasireversible processes were observed for 250 mVs^{-1} scan rate at 0.87 V(E_{pc}) and 1.0 V(E_{pa}) and for 750 mVs^{-1} at 0.9 V(E_{pc}) and 1.12 V(E_{pa}). The rest of the peaks observed for different scan rates can be said to be irreversible. The cv graphics of cobalt(II) complex of this ligand shows reversible redox processes for the scan rates 100, 500, and 750 mVs^{-1}; for example, for 500 mVs^{-1} (Figure 2(b)), the $I_{pc} : I_{pa}$ ratio equals 0.9 $\cong$ 1 (E_{pc} = 0.93 V and E_{pa} = 1.03 V). The other peak potentials recorded for this complex gave either quasireversible or irreversible redoxes. The manganese(II) complex of the same ligand gave reversible processes for the scan rates 100, 250, and 500 mVs^{-1}; for example, for 100 mVs^{-1} at 0.98 V(E_{pc}) and at 1.07 V(E_{pa}), $I_{pc} : I_{pa}$ ratio equals around 1. The other ligand, L^2, revealed reversible redoxes for scan rates 250, 500, 750, and 1000 mVs^{-1}. For example, the scan rate 750 mVs^{-1} (Figure 3(a)) gave cathodic peak potential at 0.98 V and anodic peak potential at 0.99 ($I_{pc} : I_{pa}$=1). The cobalt complex of this ligand showed reversible redoxes for 100 and 250 mVs^{-1} (Figure 3(b)) scan rates at 1.13 V(E_{pc}) and 1.1 V(E_{pa}) and at 0.99 V(E_{pc}) and 1.1 V(E_{pa}), respectively. The manganese(II) complex of the same ligand gave reversible processes for 100 and 500 mVs^{-1}. The rest of the data can be seen in Table 1. The redox processes for all the complexes can be defined as the formation of M(II) or M(I) with a simple one-electron process [24, 25]. The possible redox process for the ligands can be shown as in Figure 4.

3.3. Thermal Analysis. Thermal gravimetric analysis was used to explore the thermal stability of these newly synthesized compounds and to verify the status of water or solvent

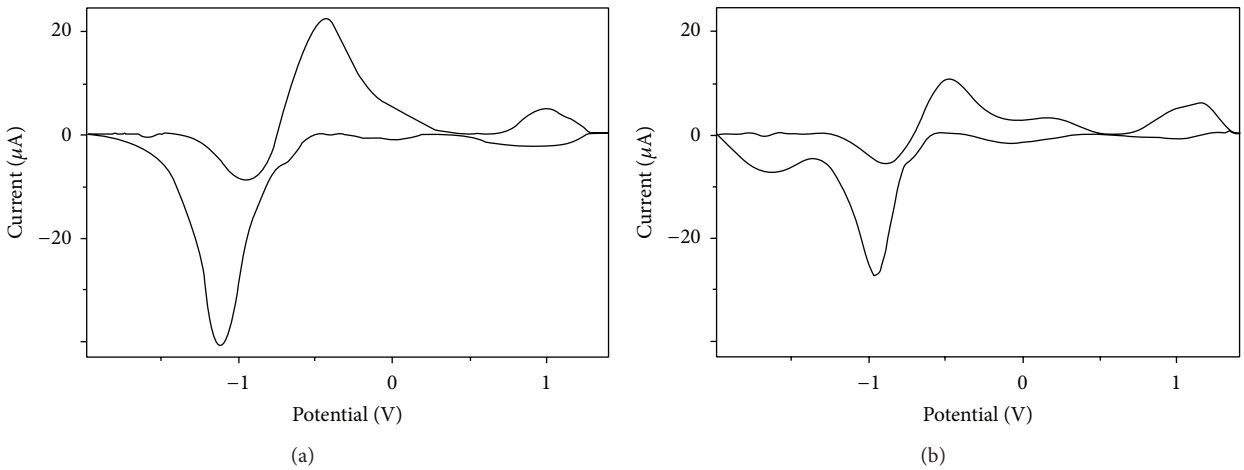

FIGURE 3: (a) Cyclic voltammogram of L^2 in the presence of 0.1 M NBu_4BF_4 in DMF solution at 1.10^{-3} M at 750 mVs^{-1}. (b) Cyclic voltammogram of L^2-Co in the presence of 0.1 M NBu_4BF_4 in DMF solution at 1.10^{-3} M at 250 mVs^{-1}.

TABLE 1: Electrochemical data of the title compounds.

Compound	Scan rate (mV/s)	E_{pc} (E_{pa}) (V)	$E_{1/2}$ (V)	ΔE_p (V)
L^1	100	0.87, −1.18 (−0.57, 0.88)	0.88	0.01
	250	0.87, −0.06, −1.24 (−0.48, 1.00)	—	0.13
	500	0.94, −0.08, −1.32 (−0.42, 1.04)	—	0.15
	750	0.90, −0.12, −1.40 (−0.38, 1.12)	—	0.22
	1000	0.90, −0.14, −1.42 (−0.35, 1.14)	—	0.24
$[Co(L^1)(H_2O)_2]2AcO$	100	0.72, −1.14 (−0.58, 0.80)	—	0.12
	250	0.76, −1.28 (−0.50, 0.93)	—	0.17
	500	0.93, −1.40 (−0.46, 1.03)	—	0.16
	750	0.97, −1.47 (−0.46, 1.07)	—	0.21
	1000	0.87, −1.54 (−0.42, 1.17)	—	0.30
$[Mn(L^1)(H_2O)_2]2AcO$	100	0.98, −1.11 (−0.52, 1.07)	—	0.09
	250	0.98, −1.13 (−0.54, 1.02)	—	0.04
	500	0.97, −1.28 (−0.40, 1.08)	—	0.13
	750	0.96, −1.41 (−0.33, 1.26)	—	0.30
	1000	0.97, −1.47 (−0.26, 1.22)	—	0.25
L^2	100	0.09, −0.90 (−0.56, −0.01, 0.82)	—	−0.10
	250	0.91, 0.03, −1.01 (−0.53, 0.93)	0.92	0.02
	500	0.94, −0.02, −1.09 (−0.50, 0.95)	0.95	0.01
	750	0.98, −1.12 (−0.44, 0.99)	0.99	0.01
	1000	0.96, −1.31 (−0.35, 0.99)	0.98	0.03
$[Co(L^2)(H_2O)_2]2AcO$	100	1.13, −0.03, −0.91 (−0.53, 0.14, 1.25)	—	0.17
	250	0.99, −0.07, −0.96 (−0.47, 0.20, 1.10)	0.72	0.12
	500	0.96, −0.08, −1.02 (−0.50, 1.13)	0.76	0.17
	750	0.95, −1.19 (−0.41, 1.10)	—	0.15
	1000	0.97, −1.42 (−0.27, 1.10)	—	0.13
$[Mn(L^2)(H_2O)_2]2AcO$	100	1.10, −0.05, −0.92 (−0.54, 1.19)	—	0.20
	250	0.96, 0.01, −1.00 (−0.49, 1.18)	0.75	0.22
	500	0.97, 0.13, −1.12 (−0.42, 1.07)	—	0.12
	750	0.96, −1.22 (−0.30, 1.11)	—	0.15
	1000	0.93, −1.43 (−0.24, 1.15)	—	0.22

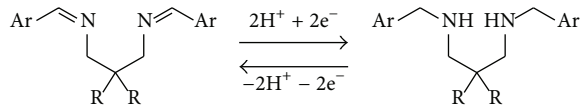

Figure 4: Reversible reduction oxidation processes of the title compounds L^1 and L^2 in DMF (1.10^{-3} M) solution.

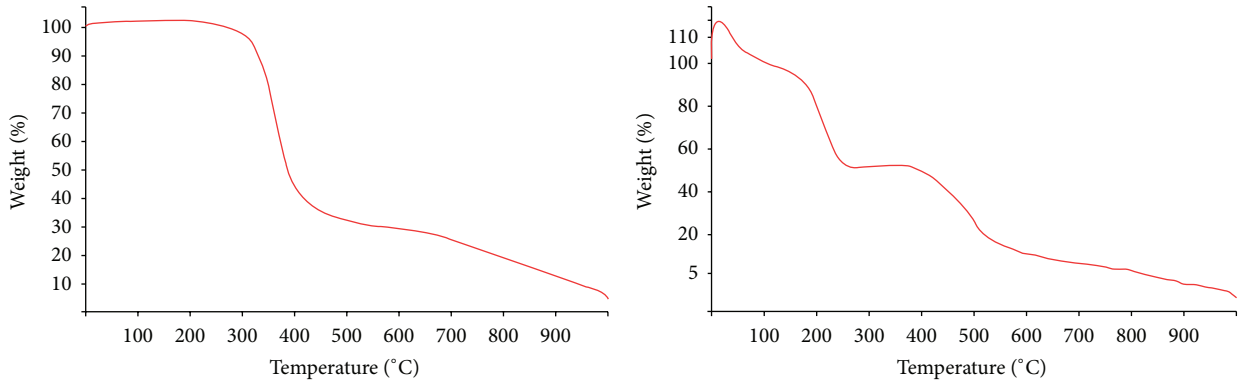

Figure 5: (a) TG plot of L^1 recorded under nitrogen atmosphere between the temperature ranges 30°C and 988°C at a heating rate of 10°C/min. (b) TG plot of L^2-Mn recorded under nitrogen atmosphere between the temperature ranges 30°C and 988°C at a heating rate of 10°C/min.

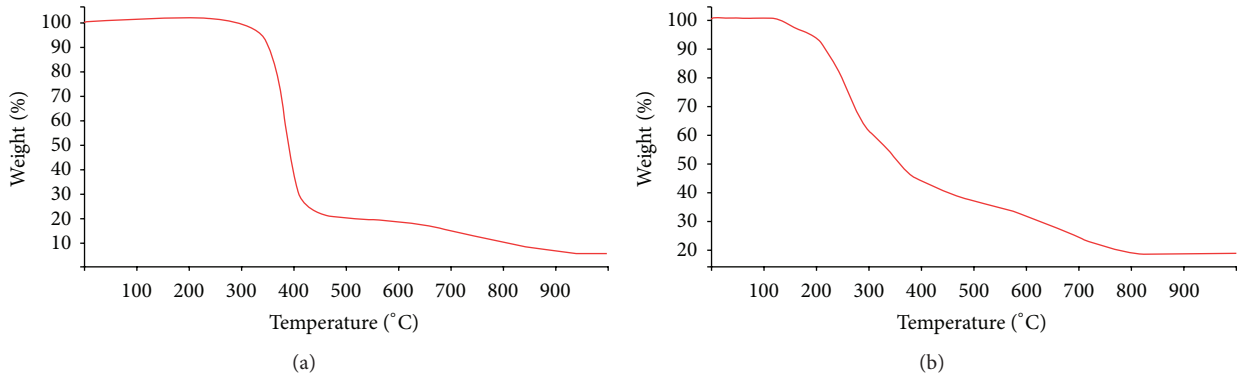

Figure 6: (a) TG plot of L^2 recorded under nitrogen atmosphere between the temperature ranges 30°C and 988°C at a heating rate of 10°C/min. (b) TG plot of L^1-Co recorded under nitrogen atmosphere between the temperature ranges 30°C and 988°C at a heating rate of 10°C/min.

molecules whether to be inside or outside of the coordination sphere of the complex compounds [26, 50]. The results of thermal analysis of the title compounds are in good agreement with the theoretical formulae as suggested from spectral analyses. The thermogram of L^1 (Figure 5(a)) shows decomposition starting around 220°C with the loss of two ethyl groups adjacent to nitrogen in the carbazole units with 12%(Calc.11.97%). The biggest loss was observed between the temperatures 340°C and 520°C with a percentage of 68.23(Calc.68%), which is assigned to the two carbazole units. The residual part was found as 19.87%(Calc.20%). One could also say that the 8.51%(Calc.8.67%) of the residual part may belong to the propyl unit which plays a bridge role between the two imine groups. TG plot of $[CoL^1(H_2O)_2]2AcO$ complex gives somewhat distorted three decomposition steps (Figure 6(b)), the first of which is observed between the temperature ranges 150°C and 220°C with a 9.2%(Calc.10%) loss belonging to the two ethyl groups on the nitrogen atoms. The second decomposition belongs to two carbazole units with a loss of 58.22%(Calc.57.35%). The third decomposition step, however, was assigned as the loss of $C_5H_8N_2$. The residual part gave percentages for metallic Co and the two water molecules. Mn(II) complex of this ligand starts to decompose at around 90°C. Between the temperatures 200°C and 430°C, our complex shows the highest percentage loss with 57.11%(Calc.57.75%) belonging to the carbazole groups. Our second ligand L^2 decomposes between the temperatures 300°C and 500°C with a total loss of 76.32%(Calc.76.17%) corresponding to the two carbazoles in our structures (Figure 6(a)). TG graphics of Mn(II) complex of L^2 (Figure 5(b)) shows three decomposition steps. The first one at 110°C corresponds to the loss of ethyl groups on the

Table 2: Thermal analysis of the ligands and their complexes.

Compound	M.W.	T/°C	Mass loss/% found (calculated)	Assignment	Residual/% found (calculated)
L^1	484.26	220–330 340–520	12.00 (11.97) 68.23 (68)	C_2H_5 $C_{12}H_8N$	19.87 (20)
$[Co_2L^1(H_2O)_2]2AcO$	579.60	150–220 220–500 500–700	9.2 (10) 58.22 (57.35) 16.17 (16.5)	C_2H_5 $C_{12}H_8N$ $C_5H_8N_2$	10.80 (10) (Co) 6.54 (6.15) (H_2O)
$[Mn_2L^1(H_2O)_2]2AcO$	575.60	90–200 200–430 430–590	10.3 (10) 57.11 (57.75) 16.8 (16.6)	C_2H_5 $C_{12}H_8N$ $C_5H_8N_2$	9.61 (9.5) (Mn) 5.94 (6.2) (H_2O)
L^2	512.69	300–500	76.32 (76.17)	$C_{14}H_{13}N$	24.04 (23.83)
$[Co_2L^2(H_2O)_2]2AcO$	607.65	200–500 830–900	54.91 (54.7) 20.48 (20.73)	$C_{12}H_8N$ $C_7H_{14}N_2$	9.48 (9.69) (Co) 5.89 (5.92) (H_2O) 9.24 (8.96) (undetermined)
$[Mn_2L^2(H_2O)_2]2AcO$	603.66	90–150 150–320 400–490	10.16 (9.6) 55.23 (55) 20.9 (20.87)	C_2H_5 $C_{12}H_8N$ $C_7H_{14}N_2$	8.48 (9.1) (Mn) 5.23 (5.43) (H_2O)

All thermal analyses were done under nitrogen atmosphere between the temperature ranges 30°C and 988°C at a heating rate of 10°C/min.

Table 3: Oxidation of styrene and cyclohexene.

Entry	Catalyst	Styrene conversion (%)	Selectivity (%)		
			Styreneoxide	Benzaldehyde	Others
1	Blank	11.5	4.5	10.0	85.5
2	$[CoL^1(H_2O)_2]2AcO$	76.7	21.8	44.5	33.7
3	$[CoL^2(H_2O)_2]2AcO$	81.3	17.4	56.1	26.5
4	$[MnL^1(H_2O)_2]2AcO$	85.3	28.2	38.9	32.9
5	$[MnL^2(H_2O)_2]2AcO$	77.8	31.8	40.5	27.7
Entry	Catalyst	Cyclohexene conversion (%)	Selectivity (%)		
			Cyclohexeneoxide	2-Cyclohexen-1-one	Others
1	Blank	17.7	7	14.3	78.7
2	$[CoL^1(H_2O)_2]2AcO$	65	14.2	61.2	24.6
3	$[CoL^2(H_2O)_2]2AcO$	69.7	18.7	58.3	23
4	$[MnL^1(H_2O)_2]2AcO$	71.2	9.3	52.4	38.3
5	$[MnL^2(H_2O)_2]2AcO$	80.9	11.2	64	24.8

Reaction conditions: alkene (10 mmol), H_2O_2 (20 mmol), catalyst (1 mmol), CH_3CN (20 mL), and nitrogen atmosphere at 90°C.

carbazoles. The second stage at 150°C corresponds to the loss of carbazole groups without the ethyls. The residual part gives a total mass loss of 13.71%(Calc.14.53%). The cobalt complex of the same ligand, however, gives the biggest mass loss of 54.91%(Calc.54.7%) between 200°C and 500°C belonging to the carbazole units. The residual part for this complex gives a total mass loss of 24.61%(Calc.24.57%), 9.24%(Calc.8.96%) of which can be assigned as the ethyl groups adjacent nitrogen on carbazole rings. The thermal data can be examined in Table 2.

3.4. Catalytic Activity. Results of the oxidation reactions (Table 3) show the catalytic activity of synthesized complexes. Comparison between neat and complex catalysed reactions proves that the oxidation reactions using catalysts give higher conversions than their corresponding neat reactions. Examination of Table 3 reveals that the coordination compounds were most effective towards the oxidation of styrene; in particular, the manganese(II) complex gave 28.2% and 31.8% selectivities for styreneoxide. Oxidation of cyclohexene, on the other hand, gave poorer results compared to those of styrene oxidation. Higher selectivities (14.2% and 18.7%) were obtained for cyclohexeneoxide by using cobalt(II) complexes as catalyst. Comparing our results to those reported previously, we can say that our compounds and their catalytic activity results, although not whole, have similarities with salen and salophane type Schiff bases reported previously [8, 12, 18, 51]. The oxidation schemes for both styrene and cyclohexene can be seen in Figure 7.

3.5. Antimicrobial Activity and Minimal Inhibitory Concentration (MIC) Analysis. The title compounds were evaluated for antimicrobial activity against four gram negative (*K. pneumoniae*, *E. aerogenes*, *E. faecium*, and *E. coli*) and four gram positive bacteria (*B. subtilis, S. aureus*, *S. S. feacalis*, and *B. megaterium*) and fungi (*C. albicans*, *C. utilis*, and *S.*

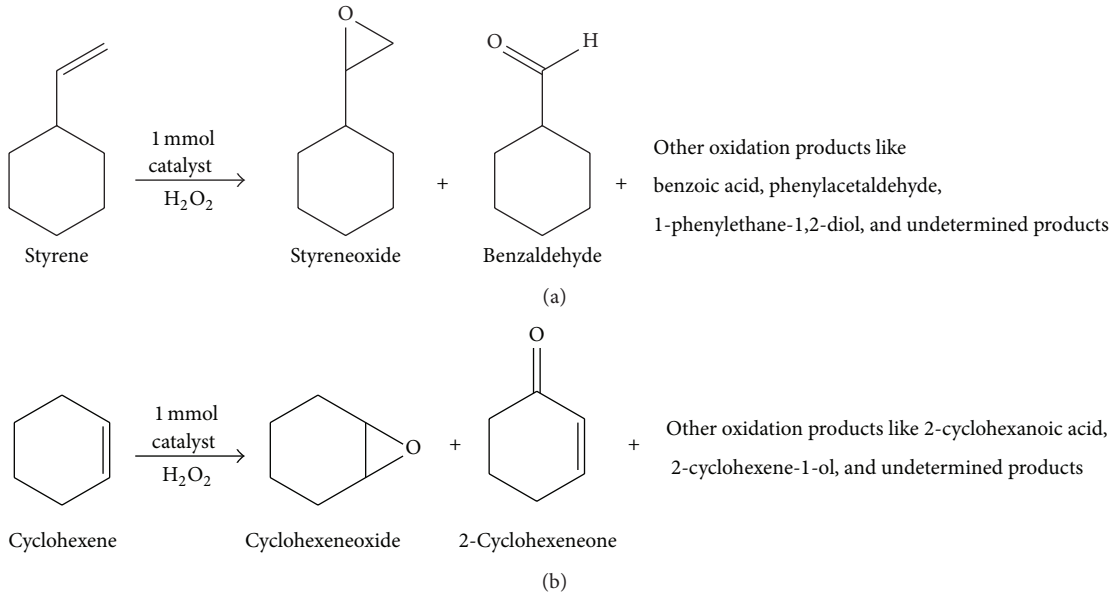

Figure 7: (a) Oxidation reaction of styrene. Catalyst : substrate : oxidant ratio: 1 : 10 : 20, under nitrogen atmosphere at 90°C. (b) Oxidation reaction of styrene. Catalyst : substrate : oxidant ratio: 1 : 10 : 20, under nitrogen atmosphere at 90°C.

Table 4: Antimicrobial data of synthesized compounds.

Microorganisms	Compounds					
	L^1	L^2	L^1–Co	L^2–Co	L^1–Mn	L^2–Mn
Gram (–)						
K. pneumoniae	18[a]	15	7	11	15	17
E. aerogenes	22	17	8	6	12	11
E. faecium	10	7	12	15	19	21
E. coli	12	11	10	9	14	16
Gram (+)						
B. subtilis	9	7	—[b]	—	8	10
S. aureus	24	21	11	9	13	12
S. faecalis	22	19	9	7	11	12
B. megaterium	15	12	—	7	11	9
Fungi						
C. albicans	11	12	—	7	9	8
C. utilis	27	25	9	10	16	17
S. cerevisiae	16	14	11	9	12	15

[a]Inhibition zone, mm.
[b]Undetermined inhibition zone.

cerevisiae). All antimicrobial and antifungal tests were performed in Mueller Hinton broth. Test tubes were incubated under normal atmospheric conditions at 37°C for 24 h for bacteria and at 30°C for 48 h for the yeasts and the microbial growth was determined by turbidimetric methods. All the synthesized compounds were effective for almost all of the microorganisms; in particular, for the microorganisms *K. pneumoniae*, *E. aerogenes*, *S. faecalis,* and *S. aureus* the title ligands brought about bigger inhibition zones. Generally, they were most effective, both antimicrobial and antifungal. Among the fungi, they gave the biggest inhibition zones for *C. utilis* with 27 mm and 25 mm zones, respectively. Among the coordination compounds, the higher values, that are both antimicrobial and antifungal, were recorded for the manganese(II) complex compounds (Table 4). Minimal inhibition zone experiments revealed that the microorganisms *K. pneumoniae*, *E. aerogenes*, *S. faecalis*, *S. aureus*, and *C. utilis* were the most sensitive microorganisms with their MIC

Table 5: MIC values of the synthesized compounds.

Microorganisms[a]	Compounds					
	L^1	L^2	L^1–Co	L^2–Co	L^1–Mn	L^2–Mn
Gram (−)						
K. pneumoniae	500	500	1000	1000	500	500
E. aerogenes	500	500	1000	1000	500	500
E. faecium	750	1000	750	750	500	500
E. coli	1000	1000	1000	1000	1000	750
Gram (+)						
B. subtilis	1000	1000	>2500	>2500	1000	1000
S. aureus	500	500	750	1000	500	500
S. faecalis	500	500	1000	1000	500	500
B. megaterium	750	1000	>2500	1000	750	1000
Fungi[b]						
C. albicans	1000	1000	>2500	1000	1000	1000
C. utilis	500	500	1000	1000	500	500
S. cerevisiae	750	750	1000	1000	750	750

[a]All microorganisms tests were performed in Mueller Hinton broth (MHB).
[b]All fungi tests were performed in Sabouraud dextrose broth (SDB).

values of 500 μg/mL to our ligands and their manganese complexes. The other microorganisms were moderately resistant to the synthesized compounds (Table 5).

4. Conclusion

With this work, carbazoles containing efficient ligands and catalysts have been synthesized, characterized, and used for the oxidation reactions of styrene and cyclohexene. Catalytic activity results show the highest selectivities for styrene oxide formation and moderate results have been obtained for the oxidation of cyclohexene. Thermal analysis results are in agreement with the proposed structures of the ligands and their coordination compounds. Thermally most stable compound is the ligand L^2 with the decomposition temperature starting at 300°C. Following this is the ligand L^1. Among the coordination compounds, cobalt complexes seem to be more resistant to temperature than manganese ones. The biological activity results reveal that both ligands and their Mn(II) complexes are effective as being antimicrobial and antifungal. The cobalt(II) complexes, however, show moderate activities. Finally, the electronic features of these compounds have also been reported.

Conflict of Interests

The authors declare that there is no conflict of interests regarding the publication of this paper.

Acknowledgment

The authors would like to thank Kahramanmaras Sutcu Imam University Research Projects Coordination Unit for the financial support.

References

[1] J. Rudolph, K. L. Reddy, J. P. Chiang, and B. K. Sharpless, "Highly efficient epoxidation of olefins using aqueous H_2O_2 and catalytic methyltrioxorhenium/pyridine: pyridine-mediated ligand acceleration," *Journal of the American Chemical Society*, vol. 119, no. 26, pp. 6189–6190, 1997.

[2] K. Sato, M. Aoki, M. Ogawa, T. Hashimoto, and R. Noyori, "A practical method for epoxidation of terminal olefins with 30% hydrogen peroxide under halide-free conditions," *Journal of Organic Chemistry*, vol. 61, no. 23, pp. 8310–8311, 1996.

[3] C. Venturello and R. DAloisio, "Quaternary ammonium tetrakis(diperoxotungsto)phosphates(3-) as a new class of catalysts for efficient alkene epoxidation with hydrogen peroxide," *Journal of Organic Chemistry*, vol. 53, pp. 1553–1557, 1988.

[4] C. Coperet, H. Adolfson, and K. B. Sharpless, "A simple and efficient method for epoxidation of terminalalkenes," *Chemical Communications*, no. 16, pp. 1565–1566, 1997.

[5] D. E. de Vos, B. F. Sels, M. Reynaers, Y. V. Subba Rao, and P. A. Jacobs, "Epoxidation of terminal or electron-deficient olefins with H_2O_2, catalysed by Mn-trimethyltriazacyclonane complexes in the presence of an oxalate buffer," *Tetrahedron Letters*, vol. 39, no. 20, pp. 3221–3224, 1998.

[6] F. Heshmatpour, S. Rayati, M. Afghan Hajiabbas, P. Abdolalian, and B. Neumüller, "Copper(II) Schiff base complexes derived from 2,2′-dimethyl- propandiamine: Synthesis, characterization and catalytic performance in the oxidation of styrene and cyclooctene," *Polyhedron*, vol. 31, no. 1, pp. 443–450, 2012.

[7] W. Zeng, J. Li, and S. Qin, "The effect of aza crown ring bearing salicylaldimine Schiff bases Mn(III) complexes as catalysts in the presence of molecular oxygen on the catalytic oxidation of styrene," *Inorganic Chemistry Communications*, vol. 9, pp. 10–12, 2006.

[8] Y. Yang, Y. Zhang, S. Hao et al., "Heterogenization of functionalized Cu(II) and VO(IV) Schiff base complexes by direct immobilization onto amino-modified SBA-15: styrene oxidation catalysts with enhanced reactivity," *Applied Catalysis A: General*, vol. 381, pp. 274–281, 2010.

[9] G. Romanowski and J. Kira, "Oxidovanadium(V) complexes with chiral tridentate Schiff bases derived from R(-)-phenylglycinol: synthesis, spectroscopic characterization and catalytic activity in the oxidation of sulfides and styrene," *Polyhedron*, vol. 53, pp. 172–178, 2013.

[10] M. Silva, C. Freire, B. de Castro, and J. L. Figueiredo, "Styrene oxidation by manganese Schiff base complexes in zeolite structures," *Journal of Molecular Catalysis A: Chemical*, vol. 258, no. 1-2, pp. 327–333, 2006.

[11] S. Rayati and F. Ashouri, "Pronounced catalytic activity of oxo-vanadium(IV) Schiff base complexes in the oxidation of cyclooctene and styrene by tert-butyl hydroperoxide," *Comptes Rendus Chimie*, vol. 15, no. 8, pp. 679–687, 2012.

[12] S. Rayati, S. Zakavi, M. Koliaei, A. Wojtczak, and A. Kozakiewicz, "Electron-rich salen-type Schiff base complexes of Cu(II) as catalysts for oxidation of cyclooctene and styrene with tert-butylhydroperoxide: a comparison with electron-deficient ones," *Inorganic Chemistry Communications*, vol. 13, no. 1, pp. 203–207, 2010.

[13] Y. Yang, J. Guan, P. Qiu, and Q. Kan, "Enhanced catalytic performances by surface silylation of Cu(II) Schiff base-containing SBA-15 in epoxidation of styrene with H_2O_2," *Applied Surface Science*, vol. 256, no. 10, pp. 3346–3351, 2010.

[14] G. Romanowski, "Synthesis, characterization and catalytic activity in the oxidation of sulfides and styrene of vanadium(V) complexes with tridentate Schiff base ligands," *Journal of Molecular Catalysis A: Chemical*, vol. 368-369, pp. 137–144, 2013.

[15] S. Mukherjee, S. Samanta, B. C. Roy, and A. Bhaumik, "Efficient allylic oxidation of cyclohexene catalyzed by immobilized Schiff base complex using peroxides as oxidants," *Applied Catalysis A: General*, vol. 301, no. 1, pp. 79–88, 2006.

[16] Y. Chang, Y. Lv, F. Lu, F. Zha, and Z. Lei, "Efficient allylic oxidation of cyclohexene with oxygen catalyzed by chloromethylated polystyrene supported tridentate Schiff-base complexes," *Journal of Molecular Catalysis A: Chemical*, vol. 320, no. 1-2, pp. 56–61, 2010.

[17] M. Salavati-Niasari and H. Babazadeh-Arani, "Cyclohexene oxidation with tert-butylhydroperoxide and hydrogen peroxide catalyzed by new square-planar manganese(II), cobalt(II), nickel(II) and copper(II) bis(2-mercaptoanil)benzil complexes supported on alumina," *Journal of Molecular Catalysis A: Chemical*, vol. 274, no. 1-2, pp. 58–64, 2007.

[18] M. Salavati-Niasari, P. Salemi, and F. Davar, "Oxidation of cyclohexene with tert-butylhydroperoxide and hydrogen peroxide catalysted by Cu(II), Ni(II), Co(II) and Mn(II) complexes of N,N′-bis-(α-methylsalicylidene)-2,2-dimethylpropane-1,3-diamine, supported on alumina," *Journal of Molecular Catalysis A: Chemical*, vol. 238, no. 1-2, pp. 215–222, 2005.

[19] M. Salavati-Niasari, M. Hassani-Kabutarkhani, and F. Davar, "Alumina-supported Mn(II), Co(II), Ni(II) and Cu(II) *N,N*-bis(salicylidene)-2,2-dimethylpropane-1,3-diamine complexes: synthesis, characterization and catalytic oxidation of cyclohexene with tert-butylhydroperoxide and hydrogen peroxide," *Catalysis Communications*, vol. 7, pp. 955–962, 2006.

[20] D. Chatterjee, S. Mukherjee, and A. Mitra, "Epoxidation of olefins with sodium hypochloride catalysed by new Nickel_II/Schiff base complexes," *Journal of Molecular Catalysis A*, vol. 154, pp. 5–8, 2000.

[21] I. Cârlescu, G. Lisa, and D. Scutaru, "Thermal stability of some ferrocene containing schiff bases," *Journal of Thermal Analysis and Calorimetry*, vol. 91, no. 2, pp. 535–540, 2008.

[22] D. Apreutesei, G. Lisa, N. Hurduc, and D. Scutaru, "Thermal behavior of some cholesteric esters," *Journal of Thermal Analysis and Calorimetry*, vol. 83, no. 2, pp. 335–340, 2006.

[23] M. Tümer, D. Ekinci, F. Tümer, and A. Bulut, "Synthesis, characterization and properties of some divalent metal(II) complexes: their electrochemical, catalytic, thermal and antimicrobial activity studies," *Spectrochimica Acta A*, vol. 67, no. 3-4, pp. 916–929, 2007.

[24] G. Ceyhan, C. Celik, S. Urus, I. Demirtas, M. Elmastas, and M. Tumer, "Antioxidant, electrochemical, thermal, antimicrobial and alkane oxidation properties of tridentate Schiff base ligands and their metal complexes," *Spectrochimica Acta Part A*, vol. 81, pp. 184–198, 2011.

[25] M. Aslantas, E. Kendi, N. Demir, A. E. Sabik, M. Tumer, and M. Kertmen, "Synthesis, spectroscopic, structural characterization, electrochemical and antimicrobial activity studies of the Schiff base ligand and its transition metal complexes," *Spectrochimica Acta A: Molecular and Biomolecular Spectroscopy*, vol. 74, no. 3, pp. 617–624, 2009.

[26] M. Shebl, "Synthesis, spectroscopic characterization and antimicrobial activity of binuclear metal complexes of a new asymmetrical Schiff base ligand: DNA binding affinity of copper(II) complexes," *Spectrochimica Acta*, vol. 117, pp. 127–137, 2014.

[27] Y.-T. Liu, G.-D. Lian, D.-W. Yin, and B.-J. Su, "Synthesis, characterization and biological activity of ferrocene-based Schiff base ligands and their metal (II) complexes," *Spectrochimica Acta A*, vol. 100, pp. 131–137, 2013.

[28] T. A. Yousef, G. M. Abu El-Reash, O. A. El-Gammal, and R. A. Bedier, "Synthesis, characterization, optical band gap, in vitro antimicrobial activity and DNA cleavage studies of some metal complexes of pyridyl thiosemicarbazone," *Journal of Molecular Structure*, vol. 1035, pp. 307–317, 2013.

[29] D. Guo, P. Wu, H. Tan, L. Xia, and W. Zhou, "Synthesis and luminescence properties of novel 4-(N-carbazole methyl) benzoyl hydrazone Schiff bases," *Journal of Luminescence*, vol. 131, no. 7, pp. 1272–1276, 2011.

[30] R. Tang, W. Zang, Y. Luo, and J. Li, "Synthesis, fluorescence properties of Eu(III) complexes with novel carbazole functionalized β-diketone ligand," *Journal of Rare Earths*, vol. 27, no. 3, pp. 362–367, 2009.

[31] S. Zhao, X. Liu, W. Feng, X. Lü, W. Wong, and W. Wong, "Effective enhancement of near-infrared emission by carbazole modification in the Zn-Nd bimetallic Schiff-base complexes," *Inorganic Chemistry Communications*, vol. 20, pp. 41–45, 2012.

[32] L. Yang, W. Zhu, M. Fang, Q. Zhang, and C. Li, "A new carbazole-based Schiff-base as fluorescent chemosensor for selective detection of Fe^{3+} and Cu^{2+}," *Spectrochimica Acta A*, vol. 109, pp. 186–192, 2013.

[33] J. Liu and J.-S. Miao, "Blue electroluminescence of a novel Zn^{2+}-β-diketone complex with a carbazole moiety," *Chinese Chemical Letters*, vol. 25, no. 1, pp. 69–72, 2014.

[34] B. Ruan, Y. Tian, H. Zhou et al., "Synthesis, characterization and in vitro antitumor activity of three organotin(IV) complexes with carbazole ligand," *Inorganica Chimica Acta*, vol. 365, no. 1, pp. 302–308, 2011.

[35] F. B. Koyuncu, S. Koyuncu, and E. Ozdemir, "A novel donor-acceptor polymeric electrochromic material containing carbazole and 1,8-naphtalimide as subunit," *Electrochimica Acta*, vol. 55, no. 17, pp. 4935–4941, 2010.

[36] S. Koyuncu, B. Gultekin, C. Zafer et al., "Electrochemical and optical properties of biphenyl bridged-dicarbazole

oligomer films: electropolymerization and electrochromism," *Electrochimica Acta*, vol. 54, no. 24, pp. 5694–5702, 2009.

[37] S. Koyuncu, C. Zafer, E. Sefer et al., "A new conducting polymer of 2,5-bis(2-thienyl)-1*H*-(pyrrole) (SNS) containing carbazole subunit: electrochemical, optical and electrochromic properties," *Synthetic Metals*, vol. 159, no. 19-20, pp. 2013–2021, 2009.

[38] Y. Liu and M. Liu, "Langmuir-Blodgett film and acidichromism of a long chain carbazole-containing Schiff base," *Thin Solid Films*, vol. 415, no. 1-2, pp. 248–252, 2002.

[39] M. Grigoras and N. Antonoaia, "Synthesis and characterization of some carbazole-based imine polymers," *European Polymer Journal*, vol. 41, no. 5, pp. 1079–1089, 2005.

[40] K. R. Yoon, S. Ko, S. M. Lee, and H. Lee, "Synthesis and characterization of carbazole derived nonlinear optical dyes," *Dyes and Pigments*, vol. 75, no. 3, pp. 567–573, 2007.

[41] NCCLS, *Performance Standards for Antimicrobial Susceptibility Testing*, M100-S9, International Supplement, Villanova, Pa, USA, 9th edition, 1999.

[42] NCCLS, *Performance Standarts for Antimicrobial Disks Susceptibilty Tests*, Approved Standart M2-A8, NCCLS, Wayne, Pa, USA, 8th edition, 2003.

[43] C. H. Collins, P. M. Lyne, and J. M. Grange, *Microbiological Methods*, Butterworths, London, UK, 1989.

[44] L. J. Bradshaw, *Laboratory Microbiology*, Saundes College Publishing, Fort Worth, Tex, USA, 4th edition, 1992.

[45] M. Tümer, C. Çelik, H. Köksal, and S. Serin, "Transition metal complexes of bidentate Schiff base ligands," *Transition Metal Chemistry*, vol. 24, pp. 525–532, 1999.

[46] E. Ispir, "The synthesis, characterization, electrochemical character, catalytic and antimicrobial activity of novel, azo-containing Schiff bases and their metal complexes," *Dyes and Pigments*, vol. 82, no. 1, pp. 13–19, 2009.

[47] M. Tümer, N. Deligönül, A. Gölcü et al., "Mixed-ligand copper(II) complexes: investigation of their spectroscopic, catalysis, antimicrobial and potentiometric properties," *Transition Metal Chemistry*, vol. 31, pp. 1–12, 2006.

[48] L. P. Nitha, R. Aswathy, N. E. Mathews, B. S. Kumari, and K. Mohanan, "Synthesis, spectroscopic characterisation, DNA cleavage, superoxidase dismutase activity and antibacterial properties of some transition metal complexes of a novel bidentate Schiff base derived from isatin and 2-aminopyrimidine," *Spectrochimica Acta A: Molecular and Biomolecular Spectroscopy*, vol. 118, pp. 154–161, 2014.

[49] N. K. Singh and S. B. Singh, "Complexes of 1-isonicotinoyl-4-benzoyl-3-thiosemicarbazide with manganese(II), iron(III), chromium(III), cobalt(II), nickel(II), copper(II) and zinc(II)," *Transition Metal Chemistry*, vol. 26, no. 4-5, pp. 487–495, 2001.

[50] H. P. Ebrahimi, J. S. Hadi, Z. A. Abdulnabi, and Z. Bolandnazar, "Spectroscopic, thermal analysis and DFT computational studies of salen-type Schiff base complexes," *Spectrochim Acta A*, vol. 117, pp. 485–492, 2014.

[51] V. Mirkhani, M. Moghadam, S. Tangestaninejad, I. Mohammadpoor-Baltork, and N. Rasouli, "Catalytic oxidation of olefins with hydrogen peroxide catalyzed by [Fe(III)(salen)Cl] complex covalently linked to polyoxometalate," *Inorganic Chemistry Communications*, vol. 10, no. 12, pp. 1537–1540, 2007.